CRYSTAL GROWTH & DESIGN

Article

pubs.acs.org/crystal

Microfluidic Approach to Cocrystal Screening of Pharmaceutical Parent Compounds

Sachit Goyal,[†] Michael R. Thorson,[†] Geoff G. Z. Zhang,[‡] Yuchuan Gong,*[,‡] and Paul J. A. Kenis*[,†]

[†]Department of Chemical & Biomolecular Engineering, University of Illinois at Urbana−Champaign, 600 South Mathews Avenue, Urbana, Illinois 61801, United States

[‡]Materials Science, Global Pharmaceutical R & D, Abbott Laboratories, 1401 Sheridan Road, NCR13-317B, North Chicago, Illinois 60064, United States

Supporting Information

ABSTRACT: We describe a microfluidic approach to screen for the formation of cocrystalline solid forms of pharmaceutical parent compounds (PCs). Saturated solutions of PCs and of cocrystal formers dissolved in a variety of solvents are precisely metered in arrays of 48 wells to enable the combinatorial mixing of all possible combinations. Key characteristics of the microfluidic approach, including small quantities (~240 μg/48 conditions), the ability to generate and screen 48 unique conditions per chip, and the ability to identify solid forms on-chip via Raman spectroscopy, enable solid form screening very early in the drug development process. In contrast, current approaches require on the order of ~240 mg for 48 conditions, thus delaying solid form screening to later stages of the drug development. Sequential screening experiments using caffeine as the model compound were conducted to validate the on-chip approach reported here. Preliminary screens were executed to identify conditions with the highest propensity for crystallization and to identify the cocrystal formers (CCFs) resulting in formation of cocrystals via on-chip Raman spectroscopy. Next, the identified, promising conditions were replicated to confirm reproducibility and consistency of the on-chip outcomes. Nine cocrystals of caffeine were identified in this way.

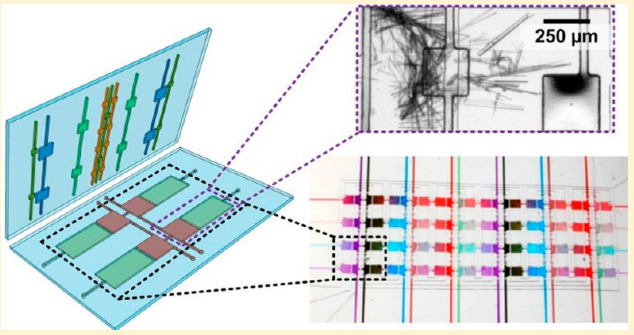

1. INTRODUCTION

Cocrystals are multicomponent assemblies held together by reversible, noncovalent interactions.[1] Cocrystallization offers a convenient way to alter the physical properties (e.g., dissolution rate, melting point, solubility, hygroscopicity) of the solid form of pharmaceutical parent compounds (PCs) without affecting their chemical identity and hence their therapeutic effects.[1−5] Cocrystal screening involves investigating a variety of cocrystal formers (CCFs), typically compounds with one or more acidic, basic, or nonionizable groups, under a variety of crystallization conditions, including choice of solvent, pH, temperature, CCF concentration, PC concentration, and PC-to-CCF ratio.[5−9] Robotic systems have been implemented to automate and thereby speed up these screening processes.[10] However, these systems require on the order of 0.5 g of PC to carry out a screen using 96-well plates, thereby preventing solid form screening in the early stages of drug development due to limited availability of PC at that time.

Typically, cocrystal screening involves direct crystallization (crystallization from clear solutions of PC and CCFs) utilizing approaches such as reactive crystallization,[9,11] temperature gradients,[12] solvent evaporation,[13] antisolvent addition, spray drying,[14] and sonochemical crystallization.[15] However, considerable differences in solubility of the components of a cocrystal hamper cocrystal formation due to too low solubility of the PC and/or the CCF. In such cases, crystallization of the PC by itself may be thermodynamically more favorable, hence preventing cocrystal formation.[16] The use of nonstoichiometric concentrations of PC and CCF, however, has been reported to result in *lower* solubility of cocrystals, and hence an improved chance for cocrystal formation.[17,18] Other methods including solid state grinding,[19,20] neat and liquid assisted grinding,[19,21] solvent drop grinding,[22] slurry conversion (solution-mediated phase transformation),[16] melt crystallization, differential scanning calorimetry,[23] and hot stage microscopy[24] have avoided some of the problems associated with direct crystallization approaches through thermodynamics. However, these methods still require large amounts of PC for the same number of experiments that one would conduct when using a direct crystallization approach. In this study, we extensively screen for cocrystals using much smaller amounts of PC, by employing microfluidic platforms for direct crystallization of saturated solutions of CCF and PC, often in nonstoichiometric molar concentrations, in a variety of solvents.

Progress in microfluidics over the last few decades has resulted in the development of large scale integrated micro-

Received: August 5, 2012
Revised: October 22, 2012
Published: October 23, 2012

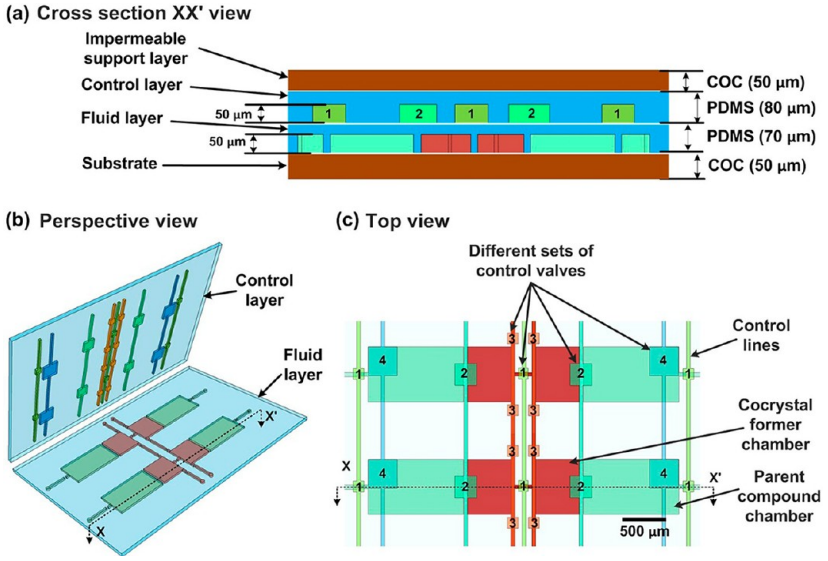

Figure 1. (a) View of cross section of four microfluidic crystallization wells (2 × 2 array) of 48 (4 × 12 array)-well multiplexed platform depicting the layered assembly of the platform. The platform comprises the PDMS fluid and control layers sandwiched between layers of cyclic olefin copolymer (COC) on top and bottom to minimize solvent loss, provide rigidity, and enable Raman compatibility. The numbers 1, 2, 3, and 4 refer to different sets of control valves. (b) Perspective view of four microfluidic crystallization wells (2 × 2 arrays) depicts parent compound and cocrystal former chambers in the fluid layer and pneumatic control lines and valves in the control layer. (c) Top view of the microfluidic platform depicts the control layer aligned over the fluid layer illustrating the function of different valves in the filling and mixing of solutions on-chip.

fluidic platforms allowing precise control over mixing and on-chip metering of solutions, on-chip detection and analysis of chemical compounds, and combinatorial mixing of very small sample sizes, thereby enabling screening of many conditions with limited material for different applications.[25−29] Specifically, microfluidic platforms find application in diverse fields such as biological studies (e.g., gene expression,[30] single cell analysis,[31] digital PCR,[32] DNA sequencing[33] and analysis[34]), point-of-care and clinical diagnostics,[35−37] and protein/pharmaceutical crystallization.[8,28,38,39] Free interface diffusion (FID) based microfluidic platforms,[25,28,39] droplet based microfluidics,[40−43] evaporation-based platforms,[44] and slip-chip approaches[45,46] have been developed to crystallize proteins as well as salts and polymorphs of PCs, and they have been used to study crystallization kinetics. However, most of the microfluidic crystallization tools reported to date have two major limitations: (1) the materials the platforms are made of are often incompatible with most of the common organic solvents,[47] and (2) they are not amenable to on-chip solid form analysis. Typically, manual harvesting of crystals is needed for analysis using techniques such as X-ray diffraction, Raman spectroscopy, solid state NMR, and/or IR spectroscopy (FTIR, near IR). Recently, we reported on a microfluidic platform for pharmaceutical salt screening that is compatible with water, alcohols, and dimethylsulfoxide (DMSO) and allows for on-chip solid form analysis via Raman spectroscopy.[28] Use of gold-coated glass substrates was needed to suppress excessive background in Raman spectra, resulting in acceptable signal-to-noise ratios.

In this study, we report a microfluidic approach that (1) enables extensive and systematic cocrystal screening with limited quantities of PCs (~240 μg per 48 conditions) via combinatorial mixing; (2) is compatible with solvents that are often used in pharmaceutical crystallization, i.e., water, alcohols, and acetonitrile; and (3) allows for on-chip solid form analysis using Raman spectroscopy. We validate this microfluidic approach through cocrystal screening of caffeine.

2. EXPERIMENTAL SECTION

Chip Assembly. The crystallization platform comprises thin polydimethylsiloxane (PDMS, General Electric RTV 615, Part A/B) fluid and control layers sandwiched between a cyclic olefin copolymer (COC, 6013 grade, TOPAS Advanced Polymers) support layer and a COC substrate layer. The fluid layer (FL) and the control layer (CL) molds were created via patterning of SU-8 2050 photoresist (MicroChem) onto silicon wafers (University wafer) to a thickness of 50 μm, each using standard photolithography.[26,48] The master molds were evaporated with a monolayer of tridecafluoro-1,1,2,2-tetrahydrooctyl)trichlorosilane (Gelest). CL (80 μm) and FL (70 μm) were obtained by spin coating 5:1 A:B, PDMS and 15:1 A:B, PDMS at 1100 and 1200 rpm respectively. The CL and the FL were partially cured on a digital hot plate/stirrer (Dataplate 730 series, Barnstead Thermolyne) at 80 °C for approximately 5 and 15 min respectively. A 2 mil (50 μm) COC sheet was bonded irreversibly to the top of the CL mold after treatment with an oxygen plasma in a plasma cleaner (Harrick Plasma) for 1 min. The COC-CL assembly was then heated at 80 °C for 10 min on a hot plate. The COC-CL assembly was carefully lifted off the CL master. The embossed side of the PDMS CL was covered with Scotch removable tape (3M) and through holes were drilled (Dremel 300 series drill with a 750 μm McMaster-Carr drill bit) to create inlets for vacuum actuation. The COC-CL assembly was manually aligned and placed on the FL under an optical microscope (Leica MZ6), followed by heating at 80 °C for 20−30 min on a hot plate to bond the layers. After the three-layer assembly was lifted off the FL master, the FL side was covered with Scotch removable tape (3M). Through-holes were drilled at the locations of the inlets and outlets in the FL. Subsequently, a 3−5 mm thick PDMS layer (5:1 A:B) was irreversibly bonded to the top of the three-layer (COC-CL-FL) assembly covering the FL and the CL inlets, after treatment with an oxygen plasma for 1 min. Through-holes were punched into the thick PDMS layer with a 20-gauge needle (BD PrecisionGlide) through the holes already drilled at the CL and the FL inlets. The complete assembly, as schematically shown in Figure 1a,b, was then reversibly bonded to a flat 2 mil COC substrate prior to setting up of the pharmaceutical solid form screening experiment. Since negative pressure was used for the operation of the valves incorporated in the device, the FL did not need to be bonded irreversibly to the COC substrate.[27,28,49]

dx.doi.org/10.1021/cg3011212 | Cryst. Growth Des. 2012, 12, 6023−6034

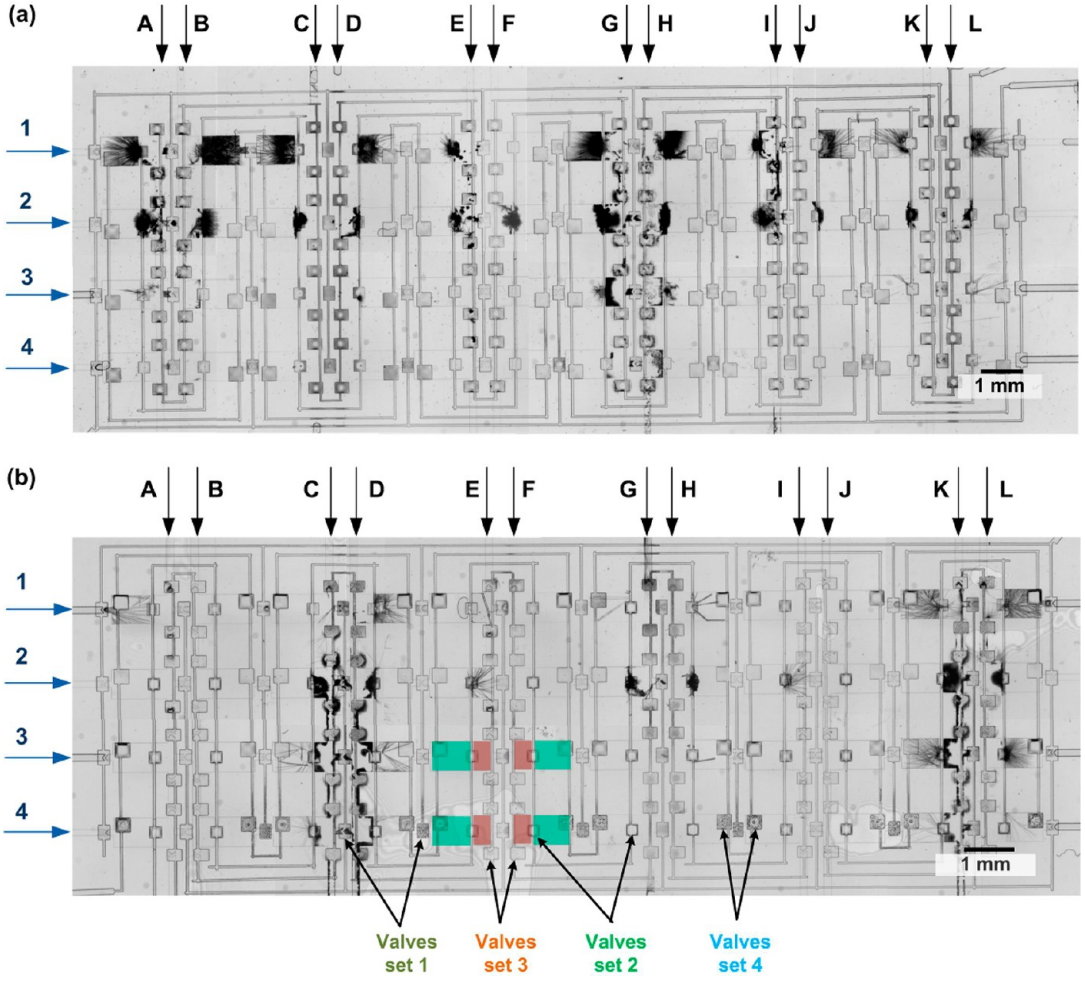

Figure 2. Tiled optical micrographs (taken 4−12 h after mixing) for an on-chip screen of cocrystal solid forms of the PC caffeine from the first phase of screening. (a) The rows are filled with PC in acetonitrile (1), acetonitrile/water (v/v = 1/1) (2), methanol (3), and ethanol (4) respectively. The columns are filled with the following CCFs in solvent: 2,4-dihydroxy benzoic acid in acetonitrile (A), acetonitrile/water (v/v = 1/1) (B), methanol (C), and ethanol (D) respectively; 3,5-dihydroxy benzoic acid in acetonitrile (E), acetonitrile/water (v/v = 1/1) (F), methanol (G), and ethanol (H) respectively; 2,5-dihydroxy benzoic acid in acetonitrile (I), acetonitrile/water (v/v = 1/1) (J), methanol (K), and ethanol (L) respectively. (b) The rows are filled with caffeine in acetonitrile (1), acetonitrile/water (v/v = 1/1) (2), methanol (3), and ethanol (4), respectively. The columns are filled with the following CCFs in solvent: 1-hydroxy 2-naphthotic acid in acetonitrile (A), acetonitrile/water (v/v = 1/1) (B), methanol (C), and ethanol (D), respectively; 2-hydroxy 1-naphthotic acid in acetonitrile (E), acetonitrile/water (v/v = 1/1) (F), methanol (G), and ethanol (H), respectively; 3-hydroxy 2-naphthotic acid in acetonitrile (I), acetonitrile/water (v/v = 1/1) (J), methanol (K), and ethanol (L), respectively. Colored boxes indicate the parent compound (green) and the cocrystal former (red) chambers and arrows indicate the different sets of control valves.

Preparation of Parent Compound and Cocrystal Former Solutions. Caffeine and all CCFs were obtained from Sigma-Aldrich and used as received. Five classes of CCFs were used: (1) *carboxylic acids*: acetic acid, formic acid, and trifluoroacetic acid; (2) *dicarboxylic acids*: oxalic acid, maleic acid, malonic acid, citric acid, glutaric acid, and adipic acid; (3) *hydroxy or dihydroxy benzoic acids*: 2-hydroxy benzoic acid, 4-hydroxy benzoic acid, 2,5-dihydroxy benzoic acid, 2,3-dihydroxy benzoic acid, 2,4-dihydroxy benzoic acid, and 3,5-dihydroxy benzoic acid; (4) *amines/amides*: indole, ethylenediamine, and saccharin; and (5) *hydroxy naphthotic acids*: 1-hydroxy 2-naphthotic acid, 2-hydroxy 1-naphthotic acid, and 3-hydroxy 2-naphthotic acid.

The following procedure was used for the preparation of the saturated solutions of caffeine and CCFs. Fifty milligrams of caffeine or 50−200 mg of CCF was dispensed into a 7 mL glass vial (Kimble/Chase). Solvents (acetonitrile, acetonitrile/water (v/v = 1/1), ethanol, or methanol) were pipetted into the glass vial in increments of 200 μL till the solid was completely dissolved. After each addition, the mixture was vortexed (Maxi Mix II, Barnstead/Thermolyne), sonicated for 2 min (Branson 2510), and then allowed to sit for about 5 min. The solubility of caffeine was estimated to be 10, 25, 7, and 8 mg/mL in acetonitrile, acetonitrile/water (v/v = 1/1), ethanol, and methanol, respectively. Extra solid was added in each of the vials at the end to ensure the solution is saturated with caffeine or CCF. The suspension was filtered, and the supernatant was used in the experiments.

On-Chip Crystallization. Fluidic routing and mixing was controlled via an array of normally closed valves (four sets) incorporated in the control layer (Figure 1b,c).[27] Microcentrifuge tubes (VWR International) were filled with PC or CCF solutions and then connected to the inlets on the platform via tubing (30 AWG thin-walled PTFE, Cole Parmer) (see Figure S1 in the Supporting Information). The PC solutions are introduced horizontally by actuating the valve sets 1 and 2 (Figure 1b), and applying vacuum suction at the outlet of the row being filled. The valve sets 1 and 2 are then closed such that the PC solutions in the PC and CCF chambers adjacent to each other are isolated. The CCF chambers are then purged with acetonitrile by actuating valve set 3 (Figure 1b) to flush PC solution from the CCF chambers, followed by introduction of the CCF solutions via application of vacuum suction at the outlet of the column being filled. Subsequently, valve set 3 is closed to lock up the CCF solutions in their chambers. Next, valve set 2 is opened for about 30 min (Figure 1b) to allow mixing of the combinatorial combinations of PC and CCF solutions confined in adjacent chambers. The mixing

dx.doi.org/10.1021/cg3011212 | *Cryst. Growth Des.* 2012, 12, 6023−6034

time can be reduced to about 10 min by repeated actuation of valves 4 (Figure 1b). After the solutions were fully mixed, all tubing for pneumatic control and fluidic flow was disconnected and the chip was sealed with Crystal Clear Tape (Hampton Research HR4−511) to prevent solvent evaporation. The chip can then be moved to the solid form analysis stations. Visualization of the whole procedure of on-chip filling and mixing in 24-wells of a 48-well microfluidic platform is available as a movie in the Supporting Information.

On-Chip Solid Form Analysis. Throughout the mixing and the following 2−12 h, the wells were periodically monitored for solid formation using an automated imaging setup comprised of an optical microscope (Leica Z16 APO) equipped with an autozoom lens (Leica 10447176), a digital camera (Leica DFC280), and a motorized X-Y stage (Semprex KL66) controlled by Image Pro Plus 7.1 software (Media Cybernetics). Images of each well were acquired every 10 min by moving the automated motorized stage in a sequential fashion from well to well. Periodically birefringent images of the wells were taken using crossed polarizers.

After the completion of the on-chip crystallization experiment, the images of the crystalline solids were captured using a stereomicroscope (Leica MZ12.5) equipped with a digital camera (Leica DFC295) and a crossed polarizer. The identity of the crystalline solids was determined by Raman spectroscopy (Renishaw mircoPL/Raman microscope). The Raman spectrometer equipped with a 785 nm excitation source (Renishaw NIR 100 mW diode laser) was connected to an upright microscope (Leica DM2500M). The microfluidic chip was placed in the sample holder and individual wells in the microfluidic chip were centered in the bright field mode using low magnification (5×), followed by use of higher magnifications (20× and/or 50×). The laser is then switched on and set at 10% laser power and the Raman spectra of individual crystals were collected in the range of 500−1700 cm^{-1} by focusing to a spot size of ∼5 μm at 50× magnification with a long working distance objective in the dark field mode. Data collection was carried out at a spectral resolution of ∼0.5 cm^{-1} at 1800 gratings/mm, with the exposure time set to 40 s, and each spectrum was averaged over two accumulations.

Off-Chip Crystallization. The cocrystal screening experiments were also conducted off-chip by mixing the same saturated solutions of caffeine and CCFs at the same volumetric ratios (150 μL of CCF solution and 300 μL of caffeine solution) in 1-mL glass vials (Kimble/Chase). The mixture of solutions was vortexed, sonicated for 5 min, and then sealed by capping the glass vials to avoid solvent evaporation. The appearance of solids in the solutions was monitored over a period of 12−72 h. The solids formed were collected by centrifugation (MiniSpin plus with Rotor F-45-12-11, Eppendorf).

Off-Chip Solid Form Analysis. PXRD patterns and Raman spectra of the solids collected in the off-chip experiments were collected and used as reference in the solid form identification.

Raman Spectroscopy. The crystals were placed on a gold-coated microscope glass slide and centered in the bright field mode of the microscope using low magnification (5×), followed by use of higher magnifications (20×). The Raman spectra of the crystal were collected using a 785 nm laser at 10% laser power in the range of 500−1700 cm^{-1} by focusing to a spot size of ∼20 μm at 20× magnification. Data collection was carried out at a spectral resolution of ∼0.5 cm^{-1} at 1800 gratings/mm, with the exposure time set to 40 s, and each spectrum was averaged over two accumulations. The gold coated glass slides were prepared by evaporating a 20-nm layer of chromium followed by a 200-nm layer of gold using E-beam evaporation system (Temescal six pocket E-Beam Evaporation System).

Powder X-ray Diffraction. The solid forms crystallized off-chip was analyzed using a D5000 diffractometer (Siemens/Bruker D-5000) using Cu K_α radiation (λ = 1.54059 Å). The sample was loaded onto a sample holder and leveled with a microscope glass slide. Data collection was carried out in the 2θ range 5−35° with a step size of 0.02°. The copper anode tube (1.5 kW fine focus) voltage and amperage were set at 40 kV and 40 mA, respectively. The instrument was controlled by a computer with the Siemens DIFFRAC plus and the data were analyzed using MDI Jade 9+.

3. RESULTS AND DISCUSSION

3.1. Design and Operation of the Microfluidic Platform. *Chip Design.* The platform used here is an adaptation of the design of a microfluidic platform we reported earlier.[28] The microfluidic platform used here has 48 wells (Figure 2), where each well is comprised of an isolated chamber for a PC solution and an adjacent chamber for a CCF solution (Figure 1b). Each well is isolated from the rest of the wells using a series of normally closed valves[27,49] and can host a separate crystallization experiment (Figure 1). Here, we conduct cocrystal screening of 48 unique conditions using a single chip: four caffeine solutions with 12 CCF solutions. Each PC chamber has a size of ∼90 nL (combined volume of the PC and the CCF chamber). The dimensions of the chambers in the chip were designed such that the solutions in the adjacent chambers can be mixed on-chip by diffusion within 30 min as estimated by Fick's law, $t = x^2/(4D)$, where x is the combined length along which the two solutions are mixing and D is the diffusivity of the diffusing species.[28] Therefore, each condition screened only requires 0.90−4.5 μg of a PC with a solubility of 10−50 mg/mL in the crystallization solvent. This microfluidic platform reduces the sample requirement by a factor of more than 1000 compared to the traditional manual screening which typically requires ∼5 mg of PC per condition. Therefore, the platform developed here enables extensive solid form screening, including cocrystal screening of a given PC, at the early stages of drug development when only limited quantities of PC are available.

PCs of interest usually have higher molecular weights and lower solubilities than the commonly used CCFs. We were able to deliver the PCs and CCFs with different solubilities on-chip in approximately equivalent molar ratios by using PC chambers that are twice as large as the CCF chambers. In addition, PCs and CCFs are frequently delivered in organic solvent and water, respectively, due to their adequate solubility in those solvents. The smaller volume of the CCF chamber, to a certain extent, prevents the precipitation of PCs dissolved in organic solvents when brought in contact with aqueous solutions of CCFs due to the antisolvent effect of water.

Chip Operation. To fill the microfluidic chips we reported previously,[28] a droplet (1−2 μL) of the PC or salt former solution had to be pipetted on the inlet port of each fluid line, and introduced into the individual chambers upon actuation of the appropriate valve sets and gentle suction at the appropriate fluid outlets. Evaporation of the solvent leading to solute precipitation and even clogging of the inlets is a drawback of this sample loading method. Here, we modified the platform to allow for a more efficient solution loading procedure. The PC and CCF solutions stored in individual off-chip containers connected to the inlets on the platform via tubing were introduced to the chambers on-chip upon actuation of the appropriate set of valves while simultaneously applying gentle suction at corresponding fluidic outlets (*vide supra*). This closed system approach minimizes solvent loss.

The modified, closed sample loading method further reduced the sample requirement. Previously droplets of PC solutions prepared in volatile solvents such as methanol were pipetted over the inlets. These droplets were exposed to the ambient conditions for a short period of time before being pulled into the chambers in the microfluidic platform. However, a small droplet evaporates rapidly owing to a large surface exposed to the ambient conditions. In practice, we frequently had to add

Table 1. Cocrystal Formation Data (On-Chip and off-Chip) for the Parent Compound (PC) Caffeine from the First Phase ("×" Indicates Cocrystal Formation and "–" Indicates the Absence of Precipitation)

		Cocrystal former[a] / Solvent[b] (on-chip/off-chip)											
Screen 1 (Fig. 2a)		2,4B / A	2,4B / AW	2,4B / M	2,4B / E	3,5B / A	3,5B / AW	3,5B / M	3,5B / E	2,5B / A	2,5B / AW	2,5B / M	2,5B / E
PC Solvent	A	×/×	×/–	×/×	×/×	×/×	–/×	×/×	×/×	×/×	×/×	×/×	×/×
	AW	×/×	×/×	×/×	×/×	×/×	×/×	×/×	×/×	×/×	×/×	×/×	×/×
	M	×/–	×/×	–/×	×/×	×/–	–/×	×/×	×/×	–/–	–/–	×/×	×/×
	E	–/–	×/–	×/×	–/×	–/–	–/–	×/×	×/–	–/–	–/–	×/×	×/×
Screen 2 (Fig. 2b)		1,2N / A	1,2N / AW	1,2N / M	1,2N / E	2,1N / A	2,1N / AW	2,1N / M	2,1N / E	3,2N / A	3,2N / AW	3,2N / M	3,2N / E
PC Solvent	A	× /×	–/–	×/×	×/×	×/×	–/–	×/×	×/×	×/×	–/–	×/×	×/×
	AW	–/×	–/–	×/×	×/×	×/×	–/–	×/×	×/×	×/×	–/×	×/×	×/×
	M	–/–	–/–	×/×	×/×	–/–	–/–	–/×	×/×	–/–	–/–	×/×	×/×
	E	–/–	–/–	×/×	×/×	–/–	–/–	–/×	–/×	–/–	–/–	×/×	×/×
Screen 3		2,3B / A	2,3B / AW	2,3B / M	2,3B / E	2B / A	2B / AW	2B / M	2B / E	4B / A	4B / AW	4B / M	4B / E
PC Solvent	A	×/×	–/–	–/–	–/–	×/×	–/–	–/–	–/–	–/–	–/–	–/–	–/–
	AW	–/–	–/–	×/×	–/–	–/–	–/–	–/–	–/–	–/–	–/–	–/–	–/–
	M	–/–	–/–	–/–	–/–	–/–	–/–	–/–	–/–	–/–	–/–	–/–	–/–
	E	–/–	–/–	–/–	–/–	–/–	–/–	–/–	–/–	–/–	–/–	–/–	–/–
Screen 4		O / A	O / AW	O / M	O / E	M_1 / A	M_1 / AW	M_1 / M	M_1 / E	M_2 / A	M_2 / AW	M_2 / M	M_2 / E
PC Solvent	A	×/×	×/×	–/–	–/–	–/–	–/–	–/–	–/–	–/–	–/–	–/–	–/–
	AW	×/–	×/–	–/–	–/–	–/–	–/–	–/–	–/–	–/–	–/–	–/–	–/–
	M	–/–	×/–	–/–	–/–	–/–	–/–	–/–	–/–	–/–	–/–	–/–	–/–
	E	–/–	–/–	–/–	–/–	–/–	–/–	–/–	–/–	–/–	–/–	–/–	–/–
Screen 5		C / A	C / AW	C / M	C / E	C / A	G / AW	G / M	G / E	Ad / A	Ad / AW	Ad / M	Ad / E
PC Solvent	A	–/–	–/–	–/–	–/–	–/–	–/–	–/–	–/–	–/–	–/–	–/–	–/–
	AW	–/–	–/–	–/–	–/–	–/–	–/–	–/–	–/–	–/–	–/–	–/–	–/–
	M	–/–	–/–	–/–	–/–	–/–	–/–	–/–	–/–	–/–	–/–	–/–	–/–
	E	–/–	–/–	–/–	–/–	–/–	–/–	–/–	–/–	–/–	–/–	–/–	–/–
Screen 6		I / A	I / AW	I / M	I / E	S / A	S / AW	S / M	S / E	ED	AA	TFA	FA
PC Solvent	A	–/–	–/–	–/–	–/–	–/–	–/–	–/–	–/–	×/–	–/–	–/–	–/–
	AW	–/–	–/–	–/–	–/–	–/–	–/–	–/–	–/–	×/×	–/–	–/–	–/–
	M	–/–	–/–	–/–	–/–	–/–	–/–	–/–	–/–	–/–	–/–	–/–	–/–
	E	–/–	–/–	–/–	–/–	–/–	–/–	–/–	–/–	–/–	–/–	–/–	–/–

[a]Cocrystal formers: 4- and 2-hydroxy benzoic acid: "4B" and "2B"; 2,5-, 3,5-, 2,3-, and 2,4-dihydroxy benzoic acids: "2,5B", "3,5B", "2,3B", and "2,4B", respectively; saccharin "S"; acetic, formic, and trifluoroacetic acids: "AA", "FA", and "TFA", respectively; 3-hydroxy 2-naphthotic, 2-hydroxy 1-naphthotic, and 1-hydroxy 2-naphthotic acids: "3,2*N*", "2,1*N*", and "1,2*N*", respectively; adipic, citric, glutaric, maleic, malonic, and oxalic acids: "Ad", "C", "G", "M_1", "M_2", and "O", respectively; ethylene diamine "ED", and indole "I". [b]Solvents: acetonitrile "A"; acetonitrile/water (v/v = 1/1) "AW"; methanol "M"; ethanol "E".

large droplets of solutions to the inlets to have enough solution to be filled into the wells despite evaporation. Therefore, the sample required for a crystallization experiment using these microfluidic platforms was determined by the volume of the droplet required to fill the chambers instead of the size of the chambers in the platform. The modified, closed sample delivery method avoids solvent loss, thus removing the limitation on the reduction of the sample requirement. In addition, this design may allow us to further automate sample delivery.

Solvent Compatibility. Lee et al. studied the interaction of PDMS with a wide range of solvents. They ranked the solvents studied based on their solubility in PDMS and the degree to which they swell PDMS.[47] On the basis of this prior work, we expect that the PDMS-based platforms are compatible with solvents such as water, dimethylsulfoxide, dimethylformamide, and various alcohols. However, the PDMS will absorb these solvents and may swell by up to 9% in volume. Additionally, the solvents may evaporate from the surface of PDMS-based microfluidic chips, as PDMS is permeable to air and solvent vapor.[47] In crystallization chips, this solvent loss causes an undesired increase of supersaturation levels, which reduces the maximum length of experiments, typically to less than 2 h.

To minimize solvent absorption by bulk PDMS we reduced the total thickness of the PDMS fluid and control layer to ∼150 μm. To minimize solvent loss due to the evaporation, we sandwiched the PDMS layers between two 50 μm COC layers. COC is less permeable to the solvents of interests, is chemically more resistant to the solvents commonly used in crystallization, and it increases by less than 3% by weight when in contact with the solvents used in this study.[50] After filling, the inlets and outlets on the microfluidic platform were covered by Crystal Clear tape to further minimize solvent loss. These improvements allowed the chips to be used for much longer crystallization screening experiments (4–12 h) using a broad range of solvents, including volatile alcohols such as methanol, ethanol, isopropanol, trifluoroethanol, as well as acetonitrile.

Strong nonpolar organic solvents such as acetone, tetrahydrofuran, ethyl acetate, and hexanes, cause extensive swelling of PDMS, which results in significant changes in chamber volumes and thus poorly controlled crystallization conditions. Micro-

dx.doi.org/10.1021/cg3011212 | *Cryst. Growth Des.* 2012, 12, 6023–6034

fluidic platforms comprised of more solvent resistant materials will be required to enable on-chip crystallization involving these strong nonpolar organic solvents.

Raman Compatibility. The analytical techniques commonly used in crystal form identification include powder X-ray diffraction, single crystal X-ray diffraction, solid state NMR, IR spectroscopy, and Raman spectroscopy.[51−54] Raman spectroscopy is preferred for on-chip solid form identification because it is amenable to automated high throughput screening and can achieve high spatial resolution.[53] In our prior work using PDMS-based chips, we were able to collect reasonable Raman spectra from on-chip crystals, but only after integration of a gold-coated bottom substrate to suppress excessive background signal from the PDMS and fluorescence from the glass substrate.[28] Here, we significantly reduced the background signal and enhanced the signal-to-noise ratio by reducing the thickness of the PDMS layers to <150 μm and by incorporating thin sheets of Raman transparent COC. The change to COC-based chips also simplified chip fabrication and handling, and made microscopic visualization of crystals easier. Raman spectra of individual COC and PDMS layers, as well as an assembled but empty chip, are provided in the Supporting Information (Figure S2). In addition, the process of background correction of on-chip Raman spectra is provided there (Figure S3).

In summary, the microfluidic platform reported here allows us to conduct 48 crystallization experiments in a single chip with minimal solvent loss and enhanced solvent and Raman compatibility. These characteristics, as well as reduced sample requirements, are critical to the solid form screening (especially by cocrystallization) at the early stages of drug development when only limited quantities of PC are available and knowledge of the properties of the compounds is limited.

3.2. Cocrystal Screening of Caffeine. Caffeine has been reported to form cocrystals with a wide range of CCFs.[6,16,45,55−57] These CCFs include carboxylic acids,[6] dicarboxylic acids,[16,57,58] hydroxy or dihydroxy benzoic acids,[45] nitro benzoic acids,[55] hydroxy naphthotic acids,[56,59] and anilines.[55] We tested 21 CCFs representing dicarboxylic acids, hydroxy or dihydroxy benzoic acids, hydroxy naphthotic acids, carboxylic acids, and amines/amides. Saturated solutions of caffeine and each of the 17 solid CCFs were prepared in four solvents (acetonitrile, acetonitrile/water (v/v = 1/1), methanol, and ethanol). Four CCFs are liquid at the ambient conditions and were used directly.

First Phase of Screening. Extensive screening was conducted to identify promising crystallization conditions, i.e., those combinations of solvents and CCFs that exhibit the highest propensity to form crystalline solids of a given PC, and to identify those CCFs resulting in the formation of cocrystals on-chip via Raman spectroscopy. The saturated solutions of caffeine were introduced into the PC chambers in the microfluidic chips horizontally, while those of the CCFs (or liquid CCFs) were introduced into the CCF chambers vertically. The combinatorial mixing of the solutions of each caffeine/CCF pair allowed screening of 288 (4 caffeine solutions × 72 CCF solutions/liquids) crystallizations using a total of 6 microfluidic chips. On-chip crystallization experiments were monitored for up to 12 h postmixing. For comparison, the same crystallization experiments were repeated off-chip, at a larger scale, in 1 mL vials by direct mixing of the caffeine/CCF solutions.

Figure 2 shows the tiled optical micrographs of the two-microfluidic crystallization chip with the highest success rate from this cocrystal screen of caffeine: Solid forms were observed in 63 out of the 96 unique conditions screened in these two chips. Table 1 summarizes the results from all on-chip and off-chip experiments. Crystalline solids were observed in 25% of the conditions in both on-chip and off-chip experiments.

Off-Chip Experiments (Glass Vials). In the off-chip experiments, crystals appeared in the presence of 10 CCFs including 2,4-dihydroxy benzoic acid (2,4B), 3,5-dihydroxy benzoic acid (3,5B), 2,5-dihydroxy benzoic acid (2,5B), 1-hydroxy 2-naphthotic acid (1,2N), 2-hydroxy 1-naphthotic acid (2,1N), 3-hydroxy 2-naphthotic acid (3,2N), 2,3-dihydroxy benzoic acid (2,3B), 2-hydroxy benzoic acid (2B), oxalic acid (O), and ethylene diamine (ED). Mixing solutions of caffeine with those of the other CCFs including 4-hydroxy benzoic (4B), maleic (M_1), malonic (M_2), glutaric (G), citric (C), adipic (Ad), acetic (AA), formic (FA), and trifluoroacetic (TFA) acids as well as indole (I) and saccharin (S) did not result in precipitation though most of the CCFs used in this study (19 of 21)[6] have been reported to form cocrystal with caffeine. All the glass vials were sealed after solutions were mixed to prevent solvent evaporation. Therefore, crystallization was only possible when either the cocrystal or the individual components became supersaturated in the initial caffeine/CCF solution mixture.

On-Chip Experiments. Use of the microfluidic chips led to similar outcomes. Crystalline solids were observed in the presence of the same group of CCFs in the on-chip experiments as in the off-chip experiments. The fact that no solid formation was observed for many conditions on-chip in the 4−12 h post mixing time period suggests that solvent loss indeed is minimal in the chips reported here. The levels of supersaturation of either component (PC or CCF) and of the intended cocrystal are not sufficient to induce crystallization, and the lack of solvent loss prevents further increase of the supersaturation after complete mixing has been achieved.

On the basis of the excellent agreement between on-chip and off-chip cocrystal screening experiments, we expect the microfluidic chips (~90 nL wells, mixing via diffusion) to deliver similar results when the same screen is performed off-chip (in 1 mL vials, mixing via direct mixing) for a given compound. Furthermore, the significant reduction in the sample requirement gives the microfluidic approach a significant advantage in solid form screening in the early stages of drug development.

Solid Form Analysis. Cocrystal screening requires scientists not only to identify the conditions at which crystalline solids are formed, but also to determine the nature of the solids. The latter is important because the PC and/or CCFs may crystallize by themselves if they have a lower solubility in the solvent mixture after the solutions are mixed together, especially when the PC and CCF initially were dissolved in solvents with very different properties. Besides, either component may form a solvate or a hydrate in the solvent mixture. For these reasons, one cannot conclude that the total number of conditions that produces a solid form within a screen equals the incidence of cocrystals. So, to determine the number of cocrystals formed, individual solid forms need to be analyzed. Here we first located crystalline solids in the various chambers of the microfluidic chips using bright field microscopy, and then we further analyzed the solids using Raman spectroscopy.

The Raman spectra of caffeine, all CCFs, and all crystalline solids isolated from the off-chip experiments were collected in the range of 500−1700 cm^{-1} for comparison with the on-chip

results. In addition, the Raman spectra of the individual PDMS and COC layers, as well as of an assembled, empty chip were recorded (Figure S2) for background subtraction. An example of background subtraction and subsequent comparison of the Raman spectrum of an individual cocrystal with the spectra of caffeine alone and the corresponding CCF is provided in the Supporting Information (Figure S3). We determined the identity of the crystalline solids corresponding to each CCF by comparing their PXRD patterns to those reported in the literature, since the Raman spectra of all targeted cocrystals are not available. Specifically, the PXRD patterns for the cocrystals grown in glass vials in acetonitrile or in the mixture of acetonitrile/water (our off-chip experiments) were collected and found to be in good agreement with the PXRD patterns for the cocrystals reported in the literature suggesting that indeed the intended cocrystals are formed in our off-chip experiments. An example of such a comparison of PXRD patterns is provided in Figure S4 in the Supporting Information.

We did not take PXRD data on every solid form obtained from every PC and CCF solvent combination expected to yield a specific PC−CCF cocrystal. Instead, we confirmed the identity of those cocrystals by comparing their Raman spectra to the Raman spectrum of the cocrystal whose identity we already had confirmed using PXRD (see above). The observed excellent agreement between all Raman spectra for a given PC and CCF combination suggests that crystallization of a targeted cocrystal is independent of the solvent mixture it was grown from.

For the off-chip experiments, all crystalline solids were determined to be the targeted cocrystals of caffeine and the corresponding CCF, except those obtained in the presence of ethylene diamine (ED). Comparison of the PXRD pattern collected for the solid forms crystallized in the presence of ED with the PXRD for as-received caffeine powder reveals that only crystals of the PC caffeine formed when ED was present. Similarly, Raman spectra of the crystalline solids formed in the on-chip experiments were in agreement with the reference Raman spectra from the cocrystals obtained in the off-chip experiments. Figure 3 shows representative examples of Raman spectra of corresponding solid forms obtained on-chip and off-chip. The unique peaks in the Raman spectra distinguished different solid forms from each other and from caffeine and confirmed that on-chip and off-chip data were in agreement. These results confirm that nine cocrystals of caffeine were successfully prepared via combinatorial mixing of PC and CCF solutions using the microfluidic chips reported here.

Like in the off-chip experiments, the solid forms obtained from on-chip conditions that contained ethylene diamine turned out to be only crystals of caffeine itself, instead of the intended cocrystal as confirmed by Raman Spectroscopy (Figure S5). The precipitation of caffeine on-chip as well as off-chip suggests that caffeine has low solubility in ethylene diamine and ED behaves as an antisolvent when added to the solution of caffeine.

A closer examination of the results in Table 1 revealed that on-chip crystallization did not perfectly replicate the outcomes of the off-chip experiments for all conditions. Cocrystals were formed in a total of 82/288 conditions out of which 64 conditions produced cocrystals on-chip as well as off-chip, while 9 conditions yielded cocrystals uniquely in the microfluidic chips and the remaining 9 conditions resulted in cocrystals uniquely in the off-chip experiments. A number of factors can explain these differences in the on-chip and off-chip

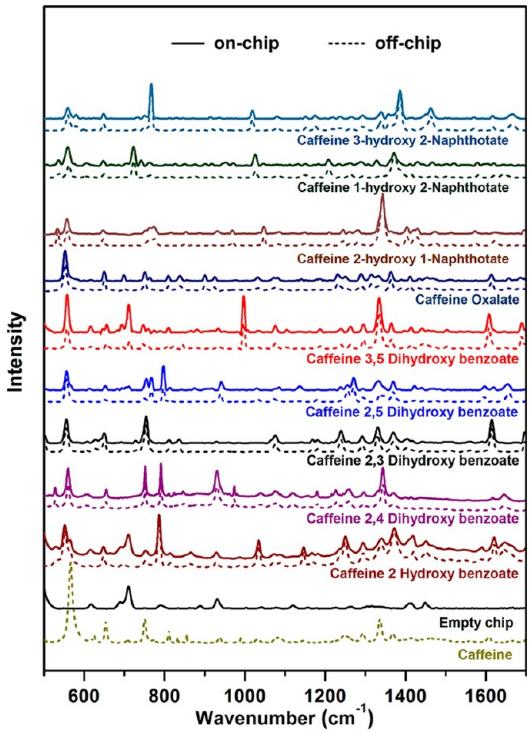

Figure 3. Raman spectroscopy data of the nine-caffeine cocrystals formed off-chip (dashed lines) and in a 48-well diffusional mixing chip (solid lines), empty microfluidic chip, and caffeine (off-chip).

crystallization outcomes: (1) *Differences in the length of the crystallization experiments.* The off-chip experiments often extended for 12−72 h, whereas most on-chip experiments were limited to 12 h or less due to considerable solvent loss encountered in the crystallization wells beyond 12 h. Beyond 12 h of experiments on-chip, we could not rely on the on-chip crystallization outcomes because then crystallization of the intended cocrystal or PC/CCF might result due to solvent evaporation (not the scope of this study) as well as reactive crystallization. The longer duration of the off-chip experiments may have led to a few more conditions resulting in solid forms resulting from slow nucleation kinetics of some of the cocrystals. Here, this is a possible explanation for 3 of the 9 cases in which solid forms were observed off-chip, but no solids were crystallized on-chip. (2) *Differences in the method of mixing of the PC and CCF solutions.* In the off-chip experiments, the solutions are brought in contact by pipetting one solution onto the other, which can result in very high supersaturation levels on contact. However, the rate of change of supersaturation level is very rapid due to instantaneous mixing attained in off-chip experiments resulting from vortexing and sonication of solutions. This convective, direct mixing process led to screening of a wide range of supersaturation levels rapidly and thereby might result in instantaneous precipitation of solids. In the on-chip experiments, the two solutions are brought into contact with each other only at the interface of the PC and CCF chamber by opening a valve, which is followed by a slow diffusive mixing process (no convection). The supersaturation level attained on-chip is defined by the relative size of the chambers or the volumetric ratios in which the solutions are mixed and the initial concentration of both the solutions.[39] On-chip diffusional mixing may lead to local supersaturation levels that are lower than those achieved by

dx.doi.org/10.1021/cg3011212 | *Cryst. Growth Des.* 2012, 12, 6023−6034

Table 2. Cocrystal Formation Data (On-Chip and off-Chip) for the Parent Compound (PC) Caffeine from the Second Phase ("×" Indicates Cocrystal Formation and "–" Indicates the Absence of Precipitation)

		Cocrystal former[a] / Solvent[b] (*on-chip/off-chip*)											
Screen 1 (Fig. 3)		2,1N / A		3,2N / A		1,2N / A		2,3B / M		O / A		ED	
PC Solvent	A	×[d]/×	×/×	×/×	×/×	×/×	×/×	–[d]/–	–/–	×/×	×/×	–/–	–/–
	A	×/×	×/×	×/×	×/×	×/×	×/×	–/–	–/–	×/×	×/×	–/–	–/–
	AW	×/×	×/×	×/×	×/×	×/×	×/×	–/×	×/×	×/×	×/×	×/×	×/×
	AW	×/×	×/×	×/×	×/×	×/×	×/×	×/×	×/×	×/×	×/×	×/×	×/×
Screen 2 (Fig. 4)		2B / A		4B / A		2,5B / A		2,4B / A		2,3B / A		3,5B / A	
PC Solvent	A	×/×	–/×	–/–	–/–	×/×	×/×	×/×	×/×	×/×	–/×	×/×	×/×
	A	×/×	–/×	–/–	–/–	×/×	×/×	×/×	×/×	–/×	–/×	×/×	×/×
	AW	–/–	–/–	–/–	–/–	×/×	×/×	×/×	×/×	–/–	–/–	×/×	×/×
	AW	–/–	–/–	–/–	–/–	×/×	×/×	–/×	×/×	–/–	–/–	×/×	×/×

[a]Cocrystal formers: 3-hydroxy 2-naphthotic acid, 2-hydroxy 1-naphthotic acid, and 1-hydroxy 2-naphthotic acids: "3,2*N*", "2,1*N*", and "1,2*N*", respectively; ethylene diamine "ED"; 2- and 4-hydroxy benzoic acids: "2B" and "4B", respectively, 3,5-, 2,5-, 2,3-, and 2,4-dihydroxy benzoic acids: "3,5B", "2,5B", "2,3B", and "2,4B", respectively; and oxalic acid "O". [b]Solvents: acetonitrile "A", acetonitrile/water (v/v = 1/1) "AW", and methanol "M".

direct mixing of solutions (off-chip) and thereby might not result in crystallization on-chip when the supersaturation level attained on-chip is low enough to lead to crystallization. However, diffusional mixing on-chip allows better control over the rate of change in supersaturation and might allow enough time at each supersaturation level, which may be conducive to crystal nucleation in some cases. Either mixing process can lead to more solid forms. Determining which crystallization outcome is due to differences in the on-chip and off-chip mixing processes is hard unless, for example, instantaneous precipitation was observed in the off-chip experiment, or in the on-chip experiment nucleation and growth is observed close to the valve location soon after the onset of mixing. (3) *Insufficient amount of one component (typically PC due to lower solubility compared to the CCFs) to generate crystals of sufficient size (depletion effect).* Each PC chamber in the microfluidic chip has a size of ∼90 nL. With the solubility of caffeine estimated as 10, 25, 7, and 8 mg/mL in acetonitrile, acetonitrile/water (v/v = 1/1), ethanol, and methanol, respectively, about 0.63−2.25 μg of caffeine is present in each of the microfluidic crystallization wells. Specifically, when the caffeine was dissolved in methanol or ethanol (only 0.63−0.72 μg caffeine present per well), crystallization of its intended cocrystal might have been difficult because of a low level of supersaturation reached after mixing. This might explain at least 4 of the 9 cases in which crystallization was observed off-chip but no solids formed on-chip. Increasing the size of the chambers might eliminate discrepancies in on-chip crystallization outcomes resulting due to delivery of an insufficient amount of one component on-chip. (4) *Imperfect formulation of crystallization conditions on-chip.* Barring a pipetting error little can go wrong in an off-chip experiment. In the on-chip experiments at times, bubbles can get trapped in a chamber or a chamber may be deformed due to a malfunctioning valve. Similarly, some PC solution may remain behind once the CCF chambers are purged after the introduction of the PC solutions preceding the introduction of the CCF solutions. In all these cases, the metering of the PC or CCF solution may be slightly off, resulting in the mixing of PC and CCF solutions in volumetric ratios different from those planned. The resulting change in solution composition and/or supersaturation level might increase or reduce the chance of crystal formation on-chip. In addition, mixing of the solutions may be insufficient at times if a valve does not open completely, or does not open at all, during the mixing process. By going through multiple generations of chip designs, most of these potential issues have been eliminated in the microfluidic platforms used for the studies reported here. Still, these issues may occur at times, causing occasional discrepancy between on- and off-chip results. (5) *The stochastic nature of crystallization reduces the probability of crystal nucleation in smaller volumes.*[8,60,61] This well-known phenomenon might explain 2 of the 9 cases in which solid forms were observed uniquely off-chip, however, extensive replication of on-chip experiments would be needed to say this with certainty. The discrepancies between the on-chip and off-chip outcomes that might occur due to the former three reasons are a result of characteristics of the microfluidic chip. However, the discrepancies that might occur due to the latter two reasons can be improved by replicating the conditions on-chip, which is feasible thanks to the limited sample requirements for on-chip experiments compared to the needs of identical off-chip experiments.

Second Phase of Screening. Cocrystal screening of caffeine was repeated in quadruplicate for several conditions to study the reproducibility and the consistency of the on-chip experiments. Caffeine crystallized with the CCFs with a higher propensity when caffeine was dissolved in acetonitrile (35% wells on-chip, 32% wells off-chip) or acetonitrile/water (33%, 32%), compared to when caffeine was dissolved in methanol (19%, 19%) and ethanol (14%, 15%). Therefore, acetonitrile-containing solvents were used for the caffeine solutions in the second phase of the study. The on-chip crystallization experiments were repeated with all 10 CCFs for which crystallization was observed. In addition, 4-hydroxy benzoic acid (4B) was used in the second phase because in the first phase caffeine crystallized with five of the six (5/6) hydroxy or dihydroxy benzoic acids screened on-chip. When caffeine was delivered in acetonitrile-containing solvents in the first round of screening, we observed that caffeine crystallized with 9/17 CCFs when the CCFs solutions were prepared in acetonitrile, with 4/17 CCFs when the CCFs solutions were prepared in 1:1 (v/v) acetonitrile/water, with 7/17 CCFs when the CCFs solutions were prepared in methanol, and with 6/17 CCFs when the CCFs solutions were prepared in ethanol. Additionally, caffeine crystallized with 1/4 liquid CCFs. Because of the

dx.doi.org/10.1021/cg3011212 | *Cryst. Growth Des.* 2012, 12, 6023−6034

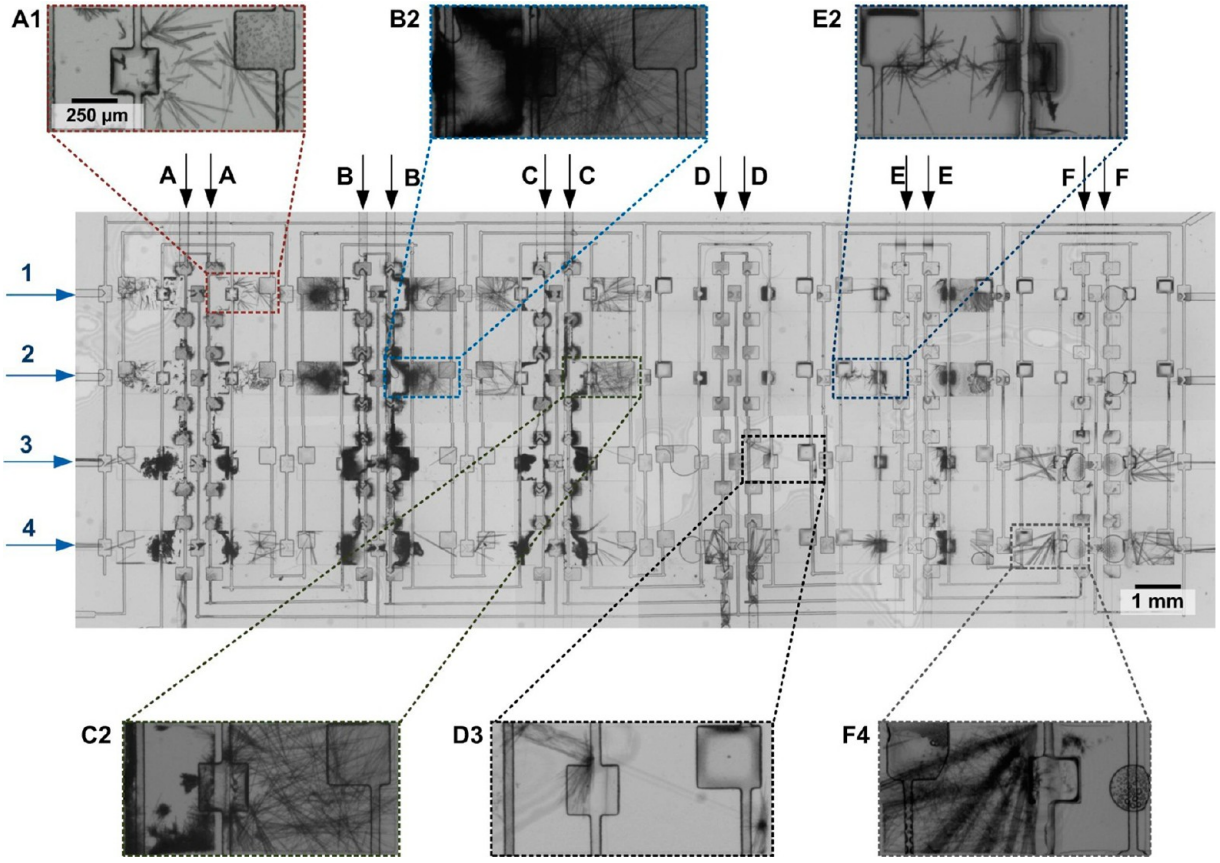

Figure 4. Tiled optical micrographs (taken 4−12 h after mixing) for an on-chip screen of cocrystal solid forms of the PC caffeine from the second phase of screening, zooming in on suitable conditions identified in the first phase of screening. (a) The rows are filled with PC in acetonitrile (1 and 2), and caffeine in acetonitrile/water (v/v = 1/1) (3 and 4). The columns are filled with the following CCFs in acetonitrile: 2-hydroxy 1-naphthotic acid (A), 3-hydroxy 2-naphthotic acid (B); 1-hydroxy 2-naphthotic acid (C); 2,3-dihydroxy benzoic acid (D) in methanol; oxalic acid (E); and ethylene diamine (F), respectively. Brightfield images of 2-hydroxy 1-naphthotate (A1); 3-hydroxy 2-naphthotate (B2); 1-hydroxy 2-naphthotate (C2); 2,3-dihydroxy benzoate (D3); oxalate (E2) cocrystals of caffeine, and the solid form of caffeine crystallized in presence of ethylene diamine (B4) are visible in the enlarged views.

high propensity of crystallization when CCFs solutions were prepared in acetonitrile and to avoid a change in solubility of either of the cocrystal screening components during mixing, we exclusively used acetonitrile as the solvent for the CCFs in the second phase. Additionally, we repeated the cocrystal screening of caffeine with 2,3-dihydroxy benzoic acid (2,3B) as the CCF in methanol since opposite results were observed when it was delivered in acetonitrile and methanol.

For each microfluidic chip in the second phase of screening, caffeine solutions prepared in acetonitrile and acetonitrile/water (v/v = 1/1) were each introduced in two adjacent rows of a 4 × 12 array chip. The six CCFs dissolved in acetonitrile were each introduced in two adjacent columns. So we screened 24 conditions in total: two 48-well chips, each with four replicates of 12 conditions. The 24 corresponding off-chip experiments were only performed once. All the solid forms crystallized on-chip were analyzed using Raman spectroscopy. The Raman spectra collected for each solid form crystallized on-chip were compared with the representative Raman spectra collected for the cocrystals obtained in the first phase of screening to confirm the identity of the solid forms.

Table 2 summarizes the results of the on-chip cocrystal screening experiments conducted during the second phase of screening, which agreed well with those from the first phase of screening (Table 1). The enlarged views in Figures 4 and 5 show typical examples of crystals formed on-chip for the conditions replicated on-chip. Caffeine formed cocrystals with all three naphthotic acids (1-hydroxy 2-naphthotic acid, 2-hydroxy 1-naphthotic acid, and 3-hydroxy 2-naphthotic acid) used in this study and oxalic acid in all crystallization wells. Caffeine also crystallized with 2,5-dihydroxy benzoic acid, 2,4-dihydroxy benzoic acid, and 3,5-dihydroxy benzoic acid, in almost all wells. Cocrystal formation of caffeine with 2,3-dihydroxy benzoic acid was observed to be dependent on the solvent. When 2,3-dihydroxy benzoic acid was delivered in acetonitrile, cocrystallization of caffeine and 2,3-dihydroxy benzoic acid only occurred when caffeine was also dissolved in acetonitrile, but not when it was dissolved in acetonitrile/water. However, water needs to be present in the acetonitrile solution of caffeine when 2,3-dihydroxy benzoic acid was dissolved in methanol. The impact of water on the cocrystal formation between caffeine and 2-hydroxy benzoic acid was also reproduced in the second screening. The cocrystal only formed when caffeine was delivered in acetonitrile, but not in the presence of water. No crystalline solid appeared in the presence of 4-hydroxy benzoic acid, in agreement with our findings during the first phase of screening. Addition of ethylene diamine to a solution of caffeine in the acetonitrile/water mixture led to the precipitation of caffeine. The agreement between the results in the first and the second

dx.doi.org/10.1021/cg3011212 | *Cryst. Growth Des.* 2012, 12, 6023−6034

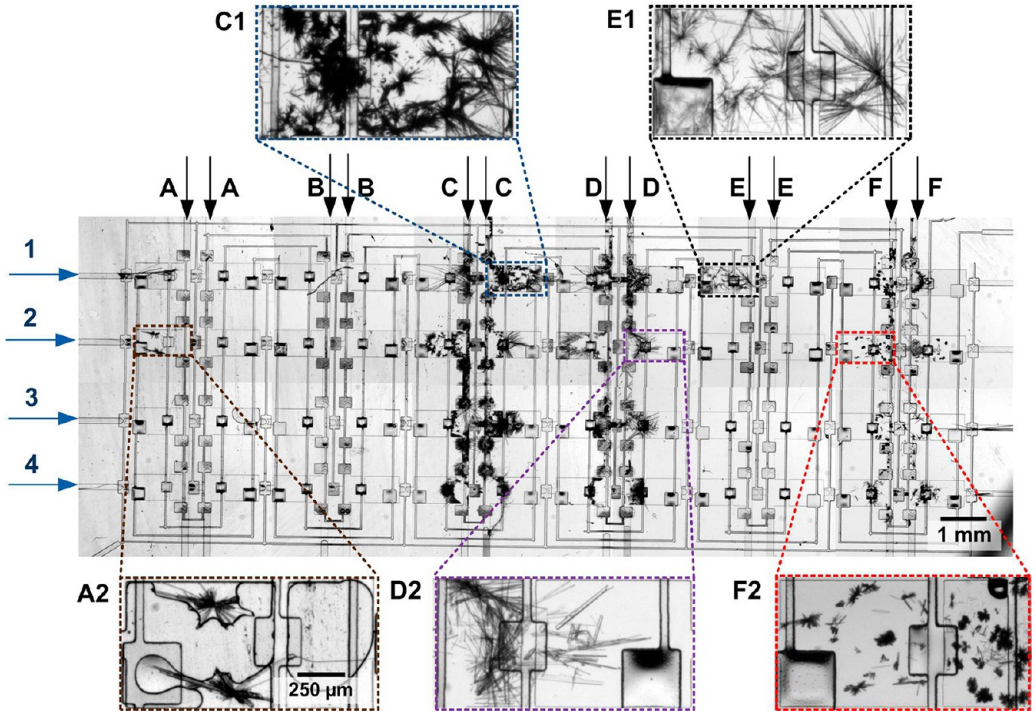

Figure 5. Tiled optical micrographs (taken 4−12 h after mixing) for an on-chip screen of cocrystal solid forms of the PC caffeine from the second phase of screening, zooming in on suitable conditions identified in the first phase of screening. (a) The rows are filled with PC in acetonitrile (1 and 2), and caffeine in acetonitrile/water (v/v = 1/1) (3 and 4). The columns are filled with the following CCFs in acetonitrile: 2-hydroxy benzoic acid (A); 4-hydroxy benzoic acid (B); 2,5-dihydroxy benzoic acid (C); 2,4-dihydroxy benzoic acid (D); 2,3-dihydroxy benzoic acid (E); and 3,5-dihydroxy benzoic acid (F) respectively. Brightfield images of 2-hydroxy benzoate (A2); 2,5-dihydroxy benzoate (C1); 2,4-dihydroxy benzoate (D2); 2,3-dihydroxy benzoate (E1); and 3,5-dihydroxy benzoate (F2) cocrystals of caffeine are visible in the enlarged views.

screening suggests that the cocrystal screening using microfluidic chips is reliable and reproducible.

Some inconsistencies in the cocrystallization outcomes were also observed in the second phase of screening. Caffeine crystallized with 2-hydroxy benzoic acid and 2,3-dihydroxy benzoic acid in 2 out of the 4 and 1 out of 4 identical experiments, respectively. Mixing caffeine dissolved in acetonitrile/water and 1-hydroxy-2-naphthotic acid dissolved in acetonitrile did not lead to cocrystal formation in the first phase of screening, but revealed a high propensity for cocrystal formation in the second phase of screening. These differences in the on-chip crystallization outcomes might be due to either the stochastic nature of crystallization especially in small volumes[8,60,61] or imperfect formulation of solutions on-chip.

Overall, these outcomes of the second phase of screening still suggest that reliable results can be obtained by replicating crystallization conditions on-chip, which is feasible thanks to the limited sample requirements for on-chip experiments compared to the needs of identical off-chip experiments.

4. CONCLUSIONS

We developed and validated hybrid COC-PDMS based microfluidic platforms for cocrystalline solid form screening of PCs. The platform meters various PC and CCF solutions and enables the creation of 48 (4 × 12 array) unique combinatorial conditions on-chip upon mixing via free interface diffusion. The use of thin PDMS layers sandwiched by COC sheets rendered the screening chips compatible with mild organic solvents typically used in pharmaceutical crystallization such as methanol, ethanol, and acetonitrile for long duration crystallization screening experiments (4−12 h). Similarly, this chip configuration is compatible with on-chip Raman analysis. The chip design, the fact that it is fully enclosed, and the way in which solutions are introduced minimize the amount of PC/CCF solution needed and avoid preconcentration of the PC/CCF solutions due to evaporation. Only ∼90 nL of solution is required for each condition screened, which represents a reduction of at least 3 orders of magnitude in sample volume compared to the conventional automated solid form screening platforms (∼500 μL per condition). The small sample size requirement allows solid form screening to be conducted at an early stage in the drug development process, at a time when only limited quantities of each PC are available. Ease of operation, requiring only a vacuum source, enables immediate application of these chips in laboratories for solid form screening. Analysis of the resulting solid forms does require a bright field microscope setup to determine size and morphology, and a Raman Spectroscopy setup for chemical identification. However, analysis can be performed separately from the screening process due to the portability and enclosed nature of the chips.

Using caffeine as the model compound, we validated the capability of the microfluidic chip to screen and identify multiple cocrystalline solid forms of PCs using only a limited amount of material. We first conducted screens to identify promising crystallization conditions, i.e., those combinations of solvents and CCFs that exhibited the highest propensity for the formation of crystalline solids of a given PC and identifying the CCFs resulting in the formation of cocrystalline solid forms on-chip via Raman spectroscopy. Subsequently, the identified promising crystallization conditions were replicated on-chip, to confirm reproducibility and consistency of the on-chip

dx.doi.org/10.1021/cg3011212 | Cryst. Growth Des. 2012, 12, 6023−6034

crystallization outcomes. The identity of the solid forms grown on-chip was confirmed by comparing their Raman spectra with those of corresponding solid forms crystallized in off-chip experiments. The COC/PDMS chips used here are also compatible with X-ray analysis and subsequent structure determination of solid forms, as we have recently shown for on-chip protein crystallization.[62]

In summary, the platform and protocol for its use presented in this paper can be applied to broad screening of suitable cocrystalline solid forms of PCs when only limited amounts of each PC are available. One can also foresee using this platform to study the effects of additives such as polymers, surfactants, and antisolvents on solid form crystallization, crystal morphology, and polymorphism of active pharmaceutical ingredients (APIs) as well as on stabilization of the amorphous forms of APIs. The solutions in these COC/PDMS-based crystallization-screening platforms are fully enclosed to minimize solvent loss. With further modifications to the current platform one could also perform crystallization screens in which solid form formation is driven by controlled evaporation of solvent. In addition, by modifying the relative dimensions of the mixing zone and the solution chambers multiple supersaturation profiles can be screened with respect to suitability for solid form crystallization. In fact, as we have shown previously for salt and polymorph screening of PCs,[28,36] the spatiotemporal variations in local concentrations of the various chemical species, and thus in local levels of supersaturation, can be modeled and correlated with crystal nucleation and growth events on-chip. The combined results of experiments and modeling will enhance understanding of what parameters determine desirable crystallization outcomes for a certain PC, which in turn will help scale up efforts in later stages of drug development, if the given PC is found to be promising for further development.

■ ASSOCIATED CONTENT

Supporting Information

Protocols for introducing solutions in the microfluidic platform, Raman spectra for all materials that the microfluidic platform is comprised of, and procedure for background correction of Raman spectrum of on-chip grown crystals, comparison of Raman spectra for off-chip and on-chip grown crystals, comparison of PXRD patterns for solid forms crystallized using our off-chip experiments to PXRD pattern for intended cocrystals available in the literature, Raman spectra for caffeine solid form crystallized in the presence of ethylene diamine, and a movie demonstrating the combinatorial mixing capability of the microfluidic platform is provided. This material is available free of charge via the Internet at http://pubs.acs.org.

■ AUTHOR INFORMATION

Corresponding Author

*(P.J.A.K.) Phone: (217) 265-0523. Fax: (217) 333-5052. E-mail: kenis@illinois.edu. Web Address: http://www.scs.uiuc.edu/~pkgroup/ (Y.G.) Phone: (847) 938-6642. Fax: (847) 937-2417. E-mail: yuchuan.gong@abbott.com.

Notes

The authors declare no competing financial interest.

■ ACKNOWLEDGMENTS

We would like to thank Abbott Laboratories for financial support. Part of this work made use of the facilities in the Micro- & Nanotechnology Laboratory as well as the Frederick Seitz Materials Research Laboratory Central Facilities at University of Illinois at Urbana−Champaign, which is partially supported by the U.S. Department of Energy under Grants DE-FG02-07ER46453 and DE-FG02-07ER46471. We thank Dr. Amit V. Desai and Dr. Daria Khvostichenko for stimulating discussions and Cassandra Schneider and Jose Gallegos-Lopez for help in fabrication of microfluidic platforms.

■ REFERENCES

(1) Good, D. J.; Rodríguez-Hornedo, N. *Cryst. Growth Des.* **2009**, *9*, 2252−2264.
(2) Childs, S. L.; Chyall, L. J.; Dunlap, J. T.; Smolenskaya, V. N.; Stahly, B. C.; Stahly, G. P. *J. Am. Chem. Soc.* **2004**, *126*, 13335−13342.
(3) Aakeroy, C. B.; Salmon, D. J. *CrystEngComm* **2005**, *7*, 439−448.
(4) Schultheiss, N.; Newman, A. *Cryst. Growth Des.* **2009**, *9*, 2950−2967.
(5) Fábián, L. s. *Cryst. Growth Des.* **2009**, *9*, 1436−1443.
(6) Musumeci, D.; Hunter, C. A.; Prohens, R.; Scuderi, S.; McCabe, J. F. *Chem. Sci.* **2011**, *2*, 883−890.
(7) Remenar, J. F.; Morissette, S. L.; Peterson, M. L.; Moulton, B.; MacPhee, J. M.; Guzman, H. R.; Almarsson, O. *J. Am. Chem. Soc.* **2003**, *125*, 8456−8457.
(8) Goh, L.; Chen, K.; Bhamidi, V.; He, G.; Kee, N. C. S.; Kenis, P. J. A.; Zukoski, C. F.; Braatz, R. D. *Cryst. Growth Des.* **2010**, *10*, 2515−2521.
(9) Childs, S. L.; Rodriguez-Hornedo, N.; Reddy, L. S.; Jayasankar, A.; Maheshwari, C.; McCausland, L.; Shipplett, R.; Stahly, B. C. *CrystEngComm* **2008**, *10*, 856−864.
(10) Desrosiers, P. J. *Modern Drug Discovery* **2004**, 40−43.
(11) Gagniere, E.; Mangin, D.; Puel, F. o.; Bebon, C.; Klein, J.-P.; Monnier, O.; Garcia, E. *Cryst. Growth Des.* **2009**, *9*, 3376−3383.
(12) ter Horst, J. H.; Deij, M. A.; Cains, P. W. *Cryst. Growth Des.* **2009**, *9*, 1531−1537.
(13) Weyna, D. R.; Shattock, T.; Vishweshwar, P.; Zaworotko, M. J. *Cryst. Growth Des.* **2009**, *9*, 1106−1123.
(14) Alhalaweh, A.; Velaga, S. P. *Cryst. Growth Des.* **2010**, *10*, 3302−3305.
(15) Friscic, T.; Childs, S. L.; Rizvi, S. A. A.; Jones, W. *CrystEngComm* **2009**, *11*, 418−426.
(16) Zhang, G. G. Z.; Henry, R. F.; Borchardt, T. B.; Lou, X. *J. Pharm. Sci.* **2007**, *96*, 990−995.
(17) Nehm, S. J.; Rodríguez-Spong, B.; Rodríguez-Hornedo, N. *Cryst. Growth Des.* **2005**, *6*, 592−600.
(18) Rodríguez-Hornedo, N.; Nehm, S. J.; Seefeldt, K. F.; Pagan-Torres, Y.; Falkiewicz, C. J. *Mol. Pharmaceutics* **2006**, *3*, 362−367.
(19) Trask, A. V.; Jones, W. Crystal Engineering of Organic Cocrystals by the Solid-State Grinding Approach. In *Organic Solid State Reactions*; Toda, F., Ed.; Springer: Berlin/Heidelberg: 2005; Vol. *254*, pp 41−70.
(20) Friscic, T.; Jones, W. *Cryst. Growth Des.* **2009**, *9*, 1621−1637.
(21) Karki, S.; Friscic, T.; Jones, W.; Motherwell, W. D. S. *Mol. Pharmaceutics* **2007**, *4*, 347−354.
(22) Trask, A. V.; Motherwell, W. D. S.; Jones, W. *Chem. Commun.* **2004**, 890−891.
(23) Lu, E.; Rodriguez-Hornedo, N.; Suryanarayanan, R. *CrystEngComm* **2008**, *10*, 665−668.
(24) Berry, D. J.; Seaton, C. C.; Clegg, W.; Harrington, R. W.; Coles, S. J.; Horton, P. N.; Hursthouse, M. B.; Storey, R.; Jones, W.; Friscic, T.; Blagden, N. *Cryst. Growth Des.* **2008**, *8*, 1697−1712.
(25) Hansen, C. L.; Skordalakes, E.; Berger, J. M.; Quake, S. R. *Proc. Natl. Acad. Sci. U. S. A.* **2002**, *99*, 16531−16536.
(26) Thorsen, T.; Maerkl, S. J.; Quake, S. R. *Science* **2002**, *298*, 580−584.
(27) Schudel, B. R.; Choi, C. J.; Cunningham, B. T.; Kenis, P. J. A. *Lab Chip* **2009**, *9*, 1676−1680.
(28) Thorson, M. R.; Goyal, S.; Schudel, B. R.; Zukoski, C. F.; Zhang, G. G. Z.; Gong, Y.; Kenis, P. J. A. *Lab Chip* **2011**, *11*, 3829−3837.

(29) Hansen, C.; Quake, S. R. *Curr. Opin. Struct. Biol.* **2003**, *13*, 538−544.
(30) Charvin, G.; Cross, F. R.; Siggia, E. D. *PLoS ONE* **2008**, *3*, e1468.
(31) Balaban, N. Q.; Merrin, J.; Chait, R.; Kowalik, L.; Leibler, S. *Science* **2004**, *305*, 1622−1625.
(32) Ottesen, E. A.; Hong, J. W.; Quake, S. R.; Leadbetter, J. R. *Science* **2006**, *314*, 1464−1467.
(33) Blazej, R. G.; Kumaresan, P.; Mathies, R. A. *Proc. Natl. Acad. Sci.. U. S. A.* **2006**, *103*, 7240−7245.
(34) Grover, W. H.; Skelley, A. M.; Liu, C. N.; Lagally, E. T.; Mathies, R. A. *Sensors Actuators B-Chem.* **2003**, *89*, 315−323.
(35) Wheeler, T. D.; Zeng, D.; Desai, A. V.; Onal, B.; Reichert, D. E.; Kenis, P. J. A. *Lab Chip* **2010**, *10*, 3387−3396.
(36) Sista, R.; Hua, Z.; Thwar, P.; Sudarsan, A.; Srinivasan, V.; Eckhardt, A.; Pollack, M.; Pamula, V. *Lab Chip* **2008**, *8*, 2091−2104.
(37) Meagher, R. J.; Hatch, A. V.; Renzi, R. F.; Singh, A. K. *Lab Chip* **2008**, *8*, 2046−2053.
(38) Perry, S. L.; Roberts, G. W.; Tice, J. D.; Gennis, R. B.; Kenis, P. J. A. *Cryst. Growth Des.* **2009**, *9*, 2566−2569.
(39) Thorson, M. R.; Goyal, S.; Gong, Y.; Zhang, G. G. Z.; Kenis, P. J. A. *CrystEngComm* **2012**, *14*, 2404−2412.
(40) Zheng, B.; Roach, L. S.; Ismagilov, R. F. *J. Am. Chem. Soc.* **2003**, *125*, 11170−11171.
(41) Zheng, B.; Gerdts, C. J.; Ismagilov, R. F. *Curr. Opin. Struct. Biol.* **2005**, *15*, 548−555.
(42) Laval, P.; Salmon, J. B.; Joanicot, M. *J. Cryst. Growth* **2007**, *303*, 622−628.
(43) Ildefonso, M.; Revalor, E.; Punniam, P.; Salmon, J. B.; Candoni, N.; Veesler, S. *J. Cryst. Growth* **2012**, *342*, 9−12.
(44) Talreja, S.; Kim, D. Y.; Mirarefi, A. Y.; Zukoski, C. F.; Kenis, P. J. A. *J. Appl. Crystallogr.* **2005**, *38*, 988−995.
(45) Bučar, D.-K. i.; Henry, R. F.; Lou, X.; Duerst, R. W.; MacGillivray, L. R.; Zhang, G. G. Z. *Cryst. Growth Des.* **2009**, *9*, 1932−1943.
(46) Li, L.; Du, W.; Ismagilov, R. F. *J. Am. Chem. Soc.* **2009**, *132*, 112−119.
(47) Lee, T.; Wang, P. Y. *Cryst. Growth Des.* **2010**, *10*, 1419−1434.
(48) Xia, Y. N.; Whitesides, G. M. *Angew. Chem., Int. Ed.* **1998**, *37*, 551−575.
(49) Mohan, R.; Schudel, B. R.; Desai, A. V.; Yearsley, J. D.; Apblett, C. A.; Kenis, P. J. A. *Sens. Actuators, B* **2011**, *160*, 1216−1223.
(50) Nunes, P. S.; Ohlsson, P. D.; Ordeig, O.; Kutter, J. P. *Microfluid. Nanofluid.* **2010**, *9*, 145−161.
(51) Allesø, M.; Velaga, S.; Alhalaweh, A.; Cornett, C.; Rasmussen, M. A.; Berg, F. v. d.; Diego, H. L. d.; Rantanen, J. *Anal. Chem.* **2008**, *80*, 7755−7764.
(52) Vogt, F. G.; Clawson, J. S.; Strohmeier, M.; Edwards, A. J.; Pham, T. N.; Watson, S. A. *Cryst. Growth Des.* **2008**, *9*, 921−937.
(53) Kojima, T.; Onoue, S.; Murase, N.; Katoh, F.; Mano, T.; Matsuda, Y. *Pharm. Res.* **2006**, *23*, 806−812.
(54) Meng, Y.; Weidner, D. J.; Gwanmesia, G. D.; Liebermann, R. C.; Vaughan, M. T.; Wang, Y.; Leinenweber, K.; Pacalo, R. E.; Yeganeh-Haeri, A.; Zhao, Y. *J. Geophys. Res.* **1993**, *98*, 22199−22207.
(55) Ghosh, S.; Malla Reddy, C. *CrystEngComm* **2012**, *14*, 2444−2453.
(56) Bučar, D.-K.; Henry, R. F.; Lou, X.; Duerst, R. W.; Borchardt, T. B.; MacGillivray, L. R.; Zhang, G. G. Z. *Mol. Pharmaceutics* **2007**, *4*, 339−346.
(57) Bucar, D.-K.; Henry, R. F.; Lou, X.; Borchardt, T. B.; Zhang, G. G. Z. *Chem. Commun.* **2007**, 525−527.
(58) Aitipamula, S.; Chow, P. S.; Tan, R. B. H. *CrystEngComm* **2012**, *14*, 2381−2385.
(59) Bučar, D.-K.; Henry, R.; Duerst, R.; Lou, X.; MacGillivray, L.; Zhang, G. *J. Chem. Crystallogr.* **2010**, *40*, 933−939.
(60) Newman, J.; Xu, J.; Willis, M. C. *Acta Crystallogr., Sect. D* **2007**, *63*, 826−832.
(61) Talreja, S.; Kenis, P. J. A.; Zukoski, C. F. *Langmuir* **2007**, *23*, 4516−4522.
(62) Guha, S.; Perry, S. L.; Pawate, A. S.; Nair, S. K.; Kenis, P. J. A. *Proceedings of the 15th International Conference on Miniaturized Systems for Chemistry and Life Sciences*; Seattle, Washington, October 2−6, 2001; Landers, Ed.; Curran Associates, Inc.: Lakeville, MN, 2012; pp 876−878.